

# Transport-driven toroidal rotation in the tokamak edge

T. Stoltzfus-Dueck\*

Max-Planck-Institut für Plasmaphysik, Boltzmannstr. 2, D-85748 Garching, Germany

The interaction of passing-ion drift orbits with spatially-inhomogeneous but purely diffusive radial transport is demonstrated to cause spontaneous toroidal spin-up to experimentally-relevant values in the tokamak edge. Physically, major-radial orbit shifts cause orbit-averaged diffusivities to depend on  $v_{\parallel}$ , including its sign, leading to residual stress. The resulting intrinsic rotation scales with  $T_i/B_{\theta}$ , resembling typical experimental scalings. Additionally, an inboard (outboard) X-point is expected to enhance co- (counter-) current rotation.

Rotation patterns strongly affected by turbulent momentum transport are broadly observed in nature, for example in atmospheric flows, stellar interiors, and accretion disks [1]. Laboratory tokamak plasmas are observed to rotate toroidally in the absence of applied torque, with edge rotation directed with the plasma current (co-current), often proportional to plasma stored energy  $W$  over plasma current  $I_p$ , and reaching tenths of the ion thermal speed  $v_{ti}$  [2, 3]. Such intrinsic rotation is of practical as well as fundamental interest, since it stabilizes certain instabilities [4] and contributes to a sheared radial electric field  $E_r$ , believed to suppress turbulent transport [5]. Intrinsic rotation is of special importance for the next-generation tokamak ITER, since  $\alpha$ -heating (nuclear fusion) applies no torque [6].

The intriguing experimental findings have triggered a broad theoretical search for the spontaneous rotation's physical origins. Although neoclassical (collisional transport) effects have been considered [7, 8], extensive experimental evidence indicates that turbulence dominates momentum transport [2, 9]. Numerical efforts have investigated turbulent momentum transport in the core, both linearly [10, 11] and nonlinearly [12]. Models for intrinsic rotation, also primarily core-focused, have treated quasilinear approximations [10, 11, 13–16], effects of inhomogeneity of the confining magnetic field  $\mathbf{B}$  [11, 14], nonresonant correlations between the fluctuating radial  $\mathbf{E} \times \mathbf{B}$  drift  $\tilde{v}_{E,r}$  and parallel velocity  $\tilde{v}_{\parallel}$  [17], and Stringer spin-up type effects [18]. Some scrape-off-layer (SOL) effects have been entertained [19, 20], but without systematic consideration of the confined plasma's response.

Momentum transport in the tokamak edge presents particular challenges for theory. The turbulence is strong, with statistics very different from quasilinear estimates [21]. It is also strongly anisotropic, with parallel fluctuation length  $L_{\parallel}$  two orders of magnitude larger than the radial length scale  $L_{\perp}$  characterizing toroidal velocity and equilibrium plasma variation [22–24]. Since parallel fluctuation gradients  $k_{\parallel} \sim 1/L_{\parallel}$  and the corresponding forces are accordingly weak, turbulently-accelerated  $\tilde{v}_{\parallel}$  and the resulting nondiffusive effects [15–17] are smaller than simple diffusive momentum transport by  $k_{\parallel} L_{\perp} \ll 1$  for realistic edge parameters. Most of these effects are further reduced, actually proportional to a “symmetry-

breaking”  $\langle k_{\parallel} \rangle \ll \langle k_{\parallel}^2 \rangle^{1/2} \sim 1/L_{\parallel}$  [16, 25]. Since  $\mathbf{B}$  varies on the scale length of the major radius  $R_0$ , the resulting momentum transport effects scale relative to simple diffusion as  $L_{\perp}/R_0 \ll 1$  in the edge [11, 14]. Further, the interaction of edge and SOL makes the problem inherently radially nonlocal. For example, the amplitude of the (unnormalized) turbulent fluctuating potential decreases in the radial direction on a short length scale  $L_{\phi} \sim L_{\perp}$  [26]. Given these experimental facts, the present work analyzes a simplified, purely-diffusive kinetic transport model, setting parallel acceleration identically to zero but retaining a model edge and SOL, passing-ion drift orbit excursions, and spatial variation of the diffusivity, finding differential transport of co- and counter-current ions to cause residual stress and consequent intrinsic rotation levels similar to those seen in experiment.

Analysis begins with a model axisymmetric drift-kinetic transport equation for the ions (c.f. [27])

$$\partial_t f_i + v \partial_y f_i - \delta v^2 (\sin y) \partial_x f_i - D(y) \partial_x (e^{-x} \partial_x f_i) = 0, \quad (1)$$

in which  $f_i(x, y, v, t)$  is the ion parallel distribution function normalized to pedestal-top ion density over thermal speed  $n_i|_{\text{pt}}/v_{ti}|_{\text{pt}}$  and  $v$  is the parallel velocity normalized to  $v_{ti}|_{\text{pt}}$ , positive for co-current motion. The geometry is simple slab plus geodesic curvature drift, with uniform poloidal  $B_{\theta}$ , toroidal  $B_{\phi}$ , and total  $B_0$  magnetic field strength. The radial position  $x$ , poloidal position  $y$ , and time  $t$  are respectively normalized to  $L_{\phi}$ , the minor radius  $a$ , and the ion transit time  $aB_0/B_{\theta}v_{ti}|_{\text{pt}}$ . The effects of nonaxisymmetric fluctuations are modeled with an inhomogeneous turbulent diffusivity, normalized to  $L_{\phi}^2 B_{\theta} v_{ti}|_{\text{pt}}/aB_0$  and assumed separable, with arbitrary poloidal dependence  $D(y)$ , decaying exponentially in  $x$ . The dimensionless parameter  $\delta \doteq q\rho_i|_{\text{pt}}/L_{\phi}$ , with  $q \doteq aB_{\phi}/R_0B_{\theta}$  the safety factor and  $\rho_i$  the thermal ion gyroradius, indicates the passing-ion orbit width relative to the radial turbulence inhomogeneity.  $\delta$  takes values around 1/4 for typical ASDEX-Upgrade (AUG) H-mode parameters [28]. Collisions are neglected, a reasonable approximation if pedestal-top ions escape without experiencing a collision, roughly for  $\nu_{ii}\tau_{\text{cr}} < 1$ , with  $\nu_{ii}$  the velocity-dependent ion collision rate and  $\tau_{\text{cr}}$  the pedestal ion stored energy over the ion heat flux. For thermal pedestal-top ions,  $\nu_{ii}\tau_{\text{cr}}$  takes values around 1

for typical H-modes in AUG, JET, and DIII-D, thus superthermal pedestal-top ions tend to exit the plasma collisionlessly while subthermal ones do not. Boundary conditions are  $f_i(-\infty, y) \rightarrow f_{i0}(v)$ ,  $f_i(\infty, y) \rightarrow 0$ ,  $f_i(x < 0, y_0) = f_i(x < 0, y_0 + 2\pi)$ ,  $f_i(x > 0, y_0, v > 0) = 0$ , and  $f_i(x > 0, y_0 + 2\pi, v < 0) = 0$ , with  $y_0$  the poloidal X-point angle. Eq. (1) is invariant to a rigid toroidal rotation  $v_{\text{rig}}$ , normalized to  $v_{ti}B_\phi/B_0$ . Although the relevant general theorem [29] does not directly apply to this non-Hamiltonian model, Eq. (1) does trivially conserve a simplified toroidal angular momentum  $\int (v + v_{\text{rig}}) f_i dv$ , as well as a density  $\int f_i dv$  and energy  $\int (1 + v^2/2) f_i dv$ .

Eq. (1) can be approximately analytically solved  $v$ -by- $v$  in steady state for both large and small  $D_{\text{eff}}$ , results agreeing for  $D_{\text{eff}} \approx 1$ . The solution procedure is briefly described here, details given in [30]. Since  $v$  appears only as a parameter,  $v$ -dependent variable transforms can greatly simplify Eq. (1). First, use new spatial variables

$$\bar{x} \doteq x - \delta v (\cos y - \cos y_0), \quad (2a)$$

$$\bar{y} \doteq D_{y0}^{-1}(v) \int_{y_0}^y D(y') e^{-\delta v (\cos y' - \cos y_0)} dy', \quad (2b)$$

with  $D_{y0}(v) \doteq \int_{y_0}^{y_0+2\pi} D(y') \exp(-\delta v (\cos y' - \cos y_0)) dy'$ . Physically,  $\bar{x}$  is a drift-surface label and  $D_{y0}$  an orbit-averaged diffusivity. Next, for  $v < 0$ , take  $\bar{y} \rightarrow 1 - \bar{y}$ . Finally, transform from  $\bar{x}$  to  $u \doteq e^{\bar{x}/2}$ , obtaining

$$\partial_{\bar{y}} f_i = (D_{\text{eff}}/4) (\partial_u^2 f_i - u^{-1} \partial_u f_i) \quad (3)$$

for  $f_i(u, \bar{y}, v)$ , in which  $D_{\text{eff}}(v) \doteq D_{y0}(v)/|v|$ . Boundary conditions are now  $f_i(0, \bar{y}) = f_{i0}(v)$ ,  $f_i(\infty, \bar{y}) \rightarrow 0$ ,  $f_i(u < 1, 0) = f_i(u < 1, 1)$ , and  $f_i(u > 1, 0) = 0$ . The normalized flux of particles with velocity  $v$  through any closed poloidal contour,  $\Gamma(v)$ , takes the simple form

$$\Gamma(v) = -\frac{1}{2} D_{y0}(v) u^{-1} \int_0^1 \partial_u f_i d\bar{y}, \quad (4)$$

evaluated at any constant  $u \leq 1$ .

Eq. (3) shows the original problem to reduce to a one-parameter family of otherwise-identical differential equations. Remarkably, the spatially-constant effective diffusivity  $D_{\text{eff}}$  depends not only on the magnitude of  $v$ , but also on its sign! Physically, as shown in Fig. 1, this results from the fact that co- (counter-) current ions' drift orbits are displaced major-radially outwards (inwards). For the typical case of turbulent diffusivities larger at the outboard, counter-current ions experience larger orbit-averaged diffusivities. Preferentially exhausting counter-current ions represents a co-current residual stress, although momentum transport at any given spatial point is purely diffusive.

In solving Eq. (3), a Laplace transform approach similar to [31] yielded the exact Green's function,

$$G(u, \xi, \tau) = \frac{2u}{D_{\text{eff}}\tau} \exp\left(-\frac{\xi^2 + u^2}{D_{\text{eff}}\tau}\right) I_1\left(\frac{2u\xi}{D_{\text{eff}}\tau}\right), \quad (5)$$

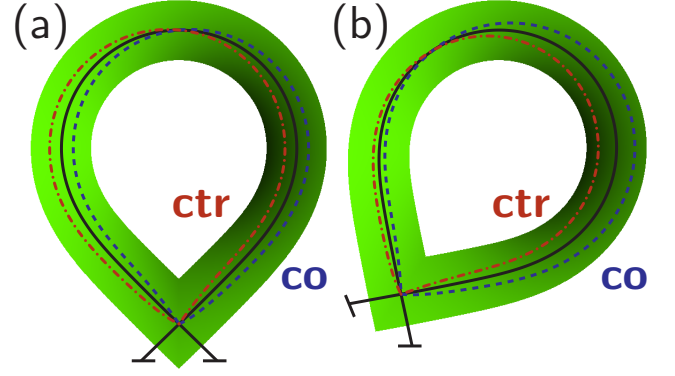


Figure 1. (color online). Co- and counter-current passing ion drift orbits over turbulence, plotted for a straight-down (a) and inboard (b) X-point. Darker shading indicates stronger diffusivity. Co- (ctr-) orbits are displaced major-radially outward (inward) as shown, regardless of the sign of  $B_\phi$  or  $I_p$ .

in terms of which the solution may be written as

$$f_i(u, \bar{y}) = f_{i0} e^{-u^2/D_{\text{eff}}\bar{y}} + \int_0^1 f_i(\xi, 0) G(u, \xi, \bar{y}) d\xi. \quad (6)$$

A first-order iterative approximation  $f_i^{(1)}$ , obtained using  $f_i(\xi, 0) \rightarrow f_{i0} \exp(-\xi^2/D_{\text{eff}})$  in Eq. (6), was demonstrated to yield an approximate normalized flux  $\Gamma/f_{i0}|v|$  with absolute error strictly less than  $\min(0.58D_{\text{eff}}^{1/2}(1 - e^{-1/D_{\text{eff}}}), 0.75/D_{\text{eff}}^{3/2})$ , tight bounds for large  $D_{\text{eff}}$ . For small  $D_{\text{eff}}$ , a two-region solution may be used, representing  $f_i$  with a Fourier series for  $u < 1$  (edge) and Laplace transforming for  $u > 1$  (SOL), requiring continuity in  $f_i$  and  $\partial_u f_i$  at  $u = 1$ , except possibly at the single point  $u = 1, \bar{y} = 0$ . The resulting edge and SOL ODEs possess explicit solutions in terms of modified Bessel functions. Slightly generalizing [32], continuity at the LCFS then requires the edge solution to satisfy

$$f_i \approx -\frac{1}{2} D_{\text{eff}}^{1/2} \frac{1}{\sqrt{\pi}} \int_0^{\bar{y}} \frac{\partial_u f_i dy'}{\sqrt{\bar{y} - y'}} - \frac{1}{8} D_{\text{eff}} \int_0^{\bar{y}} \partial_u f_i dy' \quad (7)$$

at  $u = 1$ . The resulting dense matrix for the Fourier coefficients has been solved numerically at various  $D_{\text{eff}}$ , retaining 10000 modes in  $\bar{y}$ .

The two approximate solutions,

$$\frac{\Gamma}{f_{i0}|v|} \approx \begin{cases} D_{\text{eff}} / (1 + a_1 D_{\text{eff}}^{1/2} + a_2 D_{\text{eff}}), & D_{\text{eff}} \lesssim 1 \\ -\frac{1}{2} D_{\text{eff}} \int_0^1 \partial_u f_i|_{u=1} (f_i^{(1)}/f_{i0}) d\bar{y}, & D_{\text{eff}} \gtrsim 1 \end{cases}, \quad (8)$$

are well-approximated for all  $D_{\text{eff}}$  by

$$\frac{\Gamma}{f_{i0}|v|} \approx \frac{1}{4} \ln \left( 1 + \sum_{j=2}^8 c_j D_{\text{eff}}^{j/2} \right) \approx \ln \left( 1 + \frac{D_{\text{eff}}}{e^\gamma} \right), \quad (9)$$

with  $a_1 = 0.8224$ ,  $a_2 = 0.1763$ ,  $c_2 = 4$ ,  $c_3 = -4a_1$ ,  $c_4 = 4a_1 + e^{4/(1+a_1+a_2)} - 5 - 9e^{-4\gamma}$ ,  $c_5 = c_7 = 0$ ,  $c_6 = 8e^{-4\gamma}$ ,

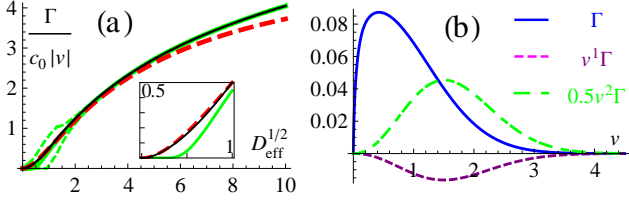


Figure 2. (color online). (a) normalized flux as a function of the  $v$ -dependent effective diffusivity, with uniform approximation (thin solid black), small- $D_{\text{eff}}$  approximation (thick dashed red), large- $D_{\text{eff}}$  approximation (thick solid green), and large- $D_{\text{eff}}$  error bounds (thin dashed green). (b) speed distribution of particle, momentum and parallel heat fluxes, assuming a Maxwellian at the inner boundary.

$c_8 = e^{-4\gamma}$ , and Euler's constant  $\gamma \approx 0.5772$ . The second approximation is used for the simplified explicit forms in Eqs. (11)–(12) and corresponding plots, the first for all other plots. The results of Eqs. (8) and (9) are plotted in Fig. 2(a), along with the large- $D_{\text{eff}}$  error bounds.

Explicit forms for normalized particle, momentum, and parallel heat fluxes may now be obtained for any specified  $f_{i0}(v)$  and  $D(y)$ . Assuming a Maxwellian  $f_{i0}(v) = e^{-v^2/2}/(2\pi)^{1/2}$  and simple ballooning form  $D(y) = D_0(1 + d_c \cos y)$ , thus

$$D_{\text{eff}}(v) = 2\pi D_0 e^{\delta v \cos y_0} [I_0(\delta v) - d_c I_1(\delta v)] / |v|, \quad (10)$$

the relevant flux moments may be reasonably approximated for small  $\delta$  as

$$\Gamma^p \doteq \int_{-\infty}^{\infty} \Gamma dv \approx \sqrt{\frac{2}{\pi}} g_1, \quad (11a)$$

$$\Pi \doteq \int_{-\infty}^{\infty} v \Gamma dv \approx 8\delta \sqrt{\frac{2}{\pi}} \left( \cos y_0 - \frac{d_c}{2} \right) (g_3 - g_5), \quad (11b)$$

$$Q_{\parallel} \doteq \int_{-\infty}^{\infty} \frac{v^2}{2} \Gamma dv \approx \sqrt{\frac{2}{\pi}} g_3, \quad (11c)$$

in which  $g_p(D_0) \doteq \ln(1 + 2\pi D_0 / e^{\gamma} p^{1/2})$ . The integrands are plotted in Fig. 2(b), summed over the sign of  $v$ . (All plots use representative AUG H-mode values  $D_0 = 0.033$ ,  $d_c = 0.8$ ,  $y_0 = -5\pi/8$ , and  $\delta = 0.28$ .)

The total momentum flux, incorporating  $v_{\text{rig}}$ , is just  $v_{\text{rig}} \Gamma^p + \Pi$ . Since toroidal rotation damping is very weak [33], a vanishing momentum input implies that momentum flux must also vanish, resulting in the pedestal-top intrinsic rotation rate

$$v_{\text{int}} = -\frac{\Pi}{\Gamma^p} \approx 8\delta (d_c/2 - \cos y_0) \frac{g_3 - g_5}{g_1}, \quad (12)$$

plotted in Fig. 3(a). Alternatively, one may balance an applied NBI torque with the outward momentum flux resulting from the NBI-driven ion heat flux. For zero

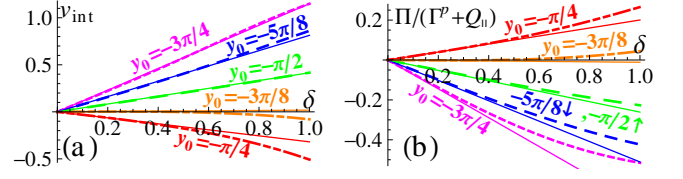


Figure 3. (color online). Normalized intrinsic rotation velocity  $v_{\text{int}}$  (a) and unbalanced NBI fraction  $\Pi / (\Gamma^p + Q_{\parallel})$  (b), plotted as functions of drift orbit width  $\delta$  for several values of poloidal X-point angle  $y_0$ , with numerical integrals (thick dashed) and analytical approximations (thin solid).

pedestal-top toroidal rotation,  $v_{\text{rig}} = 0$ , one must set the unbalanced NBI fraction  $f_{\text{unb}} \doteq (P_{\text{NBI}}^{\text{co}} - P_{\text{NBI}}^{\text{ctr}}) / P_{\text{NBI}}$  to

$$f_{\text{unb}} = \frac{f_c}{2f_{\text{NBI}}} \frac{B_{\phi}}{B_0} \frac{v_{\text{NBI}}}{v_{ti}|_{\text{pt}}} \frac{\Pi}{\Gamma^p + Q_{\parallel}}, \quad (13)$$

in which  $f_{\text{NBI}}$  is the fraction of heating by NBI,  $f_c$  is the fraction of heat transported by ions, and  $v_{\text{NBI}}$  is the beam ion velocity. The ratio  $\Pi / (\Gamma^p + Q_{\parallel})$  is plotted in Fig. 3(b). Since  $v_{\text{NBI}} / v_{ti}|_{\text{pt}}$  is typically large,  $f_{\text{unb}}$  may be a significant fraction of unity, as observed by [34].

Several features of this solution deserve comment. First, the steady-state results given in Eqs. (12)–(13) are due to a balance between large momentum transport terms [Fig. 2(b)], thus are robust. Relaxation time to the edge intrinsic rotation profile should occur roughly on an ion transport time through the pedestal,  $\sim \tau_{\text{cr}}$ . The  $v$ -asymmetric diffusion  $\Pi$  is independent of the toroidal velocity and its radial gradient, thus  $-\Pi$  represents a residual stress. For typical experimental parameters, it acts in the co-current direction with experimentally-relevant magnitude. The dimensional intrinsic rotation prediction, given here for small  $D_0$ , is

$$v_{\text{int}}^{\text{dim}} \approx 1.04 \frac{B_{\phi}}{B_0} \left( \frac{d_c}{2} - \cos y_0 \right) \frac{q \rho_i |_{\text{pt}}}{L_{\phi}} v_{ti}|_{\text{pt}} \propto \frac{T_i |_{\text{pt}}}{B_{\theta}}. \quad (14)$$

The  $1/B_{\theta}$  dependence corresponds to experimentally-observed  $1/I_p$  scalings [2, 3], while proportionality to  $T_i |_{\text{pt}}$  provides an alternative explanation for recent observations [24, 35]. Co-current spin-up at the L-H transition [2, 3] is expected due to the increase in  $T_i |_{\text{pt}}$  and probable decrease in  $L_{\phi}$ . The predicted dependence on X-point poloidal angle has yet to be experimentally tested. The physics presented here may also have implications for internal transport barrier (ITB) rotation: for outboard-ballooning and radially-increasing diffusivity (as outside an ITB), the asymmetric diffusivity results in a counter-current core rotation increment, consistent with [36, 37].

Simplifications used in this model must be kept in mind. The presented calculations omitted both the  $\nabla B$  drift and the radial electric field  $E_r$ , outside the latter's contribution to  $v_{\text{rig}}$ . While the  $\nabla B$  drift has little effect,

a uniform uncanceled poloidal  $\mathbf{E} \times \mathbf{B}$  drift of magnitude approaching  $v_{ti}B_\theta/B_0$  can represent a nonnegligible co-(counter-) residual stress for outwards (inwards)  $E_r$ , a transport effect due to a shifted relation between  $D_{y0}$  and  $D_{\text{eff}}$  [30], possibly connected with observations of a favorable/unfavorable X-point dependence of L-mode toroidal rotation [20, 37]. Treatment of sheared  $E_r$  effects or electrostatic confinement [38] would require nontrivial extensions to the theory, as would retention of collisions. Direct collisional effects on the rotation-driving flux  $\Pi$  may often be small, since  $\Pi$  results dominantly from ions that are slightly superthermal at the pedestal top [Fig. 2(b)], thus very superthermal at the LCFS, with an accordingly low collision rate. However, lower-energy ions may affect both  $E_r$  and the rotation saturation  $v_{\text{rig}}\Gamma^p$ . Finally, recall that the turbulence parameters are taken as an input to the present model, not calculated self-consistently.

In summary, radial displacements of passing-ion orbits and typical tokamak-edge turbulence inhomogeneity are shown to result in orbit-averaged diffusivities that depend on the sign of  $v_{\parallel}$ . Even in the absence of non-diffusive effects, this results in residual stress and corresponding intrinsic rotation at experimentally-relevant levels. The rotation is co-current for typical H-mode parameters and scales with  $T_{i|\text{pt}}/B_\theta$ , in agreement with experimental observations.

Helpful discussions with A. Chankin, G. Hammett, P. Helander, J. Krommes, K. Lackner, O. Maj, R. McDermott, B. Nold, T. Pütterich, C. Rost, P. Schneider, and B. Scott, and an Alexander von Humboldt Foundation research fellowship are gratefully acknowledged.

---

\* tstoltzf@ipp.mpg.de

- [1] L. L. Kichatinov, *Geophys. Astrophys. Fluid Dyn.* **35**, 93 (1986); U. Frisch, Z. S. She, and P. L. Sulem, *Physica D* **28**, 382 (1987); S. A. Balbus and J. F. Hawley, *Rev. Mod. Phys.* **70**, 1 (1998); M. S. Miesch and J. Toomre, *Annu. Rev. Fluid Mech.* **41**, 317 (2009).
- [2] J. S. deGrassie, *Plasma Phys. Controlled Fusion* **51**, 124047 (2009), and references therein.
- [3] J. E. Rice *et al.*, *Nucl. Fusion* **47**, 1618 (2007).
- [4] E. Strait *et al.*, *Phys. Rev. Lett.* **74**, 2483 (1995).
- [5] H. Biglari *et al.*, *Phys. Fluids B* **2**, 1 (1990).
- [6] E. J. Doyle *et al.*, *Nucl. Fusion* **47**, S18 (2007), Sec. 3.5.
- [7] C. S. Chang and S. Ku, *Phys. Plasmas* **15**, 062510 (2008).
- [8] A. L. Rogister *et al.*, *Nucl. Fusion* **42**, 1144 (2002); R. Singh *et al.*, *Phys. Plasmas* **13**, 042505 (2006); U. Daybelge *et al.*, *Nucl. Fusion* **49**, 115007 (2009).
- [9] S. D. Scott *et al.*, *Phys. Rev. Lett.* **64**, 531 (1990); W. D. Lee *et al.*, *ibid.* **91**, 205003 (2003); A. Kallenbach *et al.*, *Plasma Phys. Controlled Fusion* **33**, 595 (1991); J. E. Rice *et al.*, *Nucl. Fusion* **44**, 379 (2004).
- [10] R. R. Dominguez and G. M. Staebler, *Phys. Fluids B* **5**, 3876 (1993); A. G. Peeters *et al.*, *Phys. Rev. Lett.* **98**, 265003 (2007); *Phys. Plasmas* **16**, 042310 (2009); **16**, 062311 (2009); N. Kluy *et al.*, **16**, 122302 (2009).
- [11] Y. Camenen *et al.*, *Phys. Rev. Lett.* **102**, 125001 (2009); *Phys. Plasmas* **16**, 062501 (2009).
- [12] X. Garbet *et al.*, *Phys. Plasmas* **9**, 3893 (2002); R. E. Waltz *et al.*, **14**, 122507 (2007); I. Holod and Z. Lin, **15**, 092302 (2008); P. W. Terry *et al.*, **16**, 122305 (2009); W. X. Wang *et al.*, *Phys. Rev. Lett.* **102**, 035005 (2009); **106**, 085001 (2011).
- [13] K. C. Shaing, *Phys. Rev. Lett.* **86**, 640 (2001); E. S. Yoon and T. S. Hahm, *Nucl. Fusion* **50**, 064006 (2010); R. Singh *et al.*, **51**, 013002 (2011).
- [14] T. S. Hahm *et al.*, *Phys. Plasmas* **14**, 072302 (2007).
- [15] B. Coppi, *Nucl. Fusion* **42**, 1 (2002); Ö. D. Gürcan *et al.*, *Phys. Plasmas* **14**, 042306 (2007).
- [16] C. J. McDevitt *et al.*, *Phys. Rev. Lett.* **103**, 205003 (2009); *Phys. Plasmas* **16**, 052302 (2009); C. J. McDevitt and P. H. Diamond, **16**, 012301 (2009).
- [17] P. H. Diamond *et al.*, *Phys. Plasmas* **15**, 012303 (2008); *Nucl. Fusion* **49**, 045002 (2009); Ö. D. Gürcan *et al.*, *Phys. Plasmas* **17**, 112309 (2010).
- [18] H. Wobig and J. Kießlinger, *Plasma Phys. Controlled Fusion* **37**, 893 (1995); A. G. Peeters, *Phys. Plasmas* **5**, 2399 (1998); V. A. Rozhansky and I. Y. Senichenkov, *Plasma Phys. Controlled Fusion* **52**, 065003 (2010).
- [19] V. Rozhansky and M. Tendler, *Phys. Plasmas* **1**, 2711 (1994); A. V. Chankin and W. Kerner, *Nucl. Fusion* **36**, 563 (1996); V. Rozhansky *et al.*, *Plasma Phys. Reports* **34**, 730 (2008).
- [20] B. LaBombard *et al.*, *Nucl. Fusion* **44**, 1047 (2004).
- [21] M. Wakatani and A. Hasegawa, *Phys. Fluids* **27**, 611 (1984); B. D. Scott, *Phys. Plasmas* **12**, 062314 (2005).
- [22] M. Endler, *J. Nucl. Mater.* **266–269**, 84 (1999); J. Bleuel *et al.*, *New Journal of Physics* **4**, 38 (2002).
- [23] T. Pütterich *et al.*, *Phys. Rev. Lett.* **102**, 025001 (2009).
- [24] J. S. deGrassie *et al.*, *Nucl. Fusion* **49**, 085020 (2009).
- [25] A. G. Peeters and C. Angioni, *Phys. Plasmas* **12**, 072515 (2005).
- [26] C. P. Ritz *et al.*, *Phys. Rev. Lett.* **65**, 2543 (1990); M. Endler *et al.*, *Nucl. Fusion* **35**, 1307 (1995); R. A. Moyer *et al.*, *J. Nucl. Mater.* **241–243**, 633 (1997); **266–269**, 1145 (1999); C. Silva *et al.*, *Rev. Sci. Instrum.* **75**, 4314 (2004); B. LaBombard *et al.*, *Nucl. Fusion* **45**, 1658 (2005); J. Horacek *et al.*, **50**, 105001 (2010).
- [27] P. J. Catto and R. D. Hazeltine, *Phys. Plasmas* **1**, 1882 (1994).
- [28] T. Pütterich, P. Schneider, and E. Wolfrum (private communication).
- [29] B. Scott and J. Smirnov, *Phys. Plasmas* **17**, 112302 (2010); A. J. Brizard and N. Tronko, (submitted).
- [30] T. Stoltzfus-Dueck, (work in preparation).
- [31] L. Farnell and W. G. Gibson, *J. Comput. Phys.* **198**, 65 (2004), App. A.1.
- [32] K. B. Oldham and J. Spanier, *J. Math. Anal. Appl.* **39**, 655 (1972).
- [33] J. W. Connor *et al.*, *Plasma Phys. Controlled Fusion* **29**, 919 (1987).
- [34] W. M. Solomon *et al.*, *Plasma Phys. Controlled Fusion* **49**, B313 (2007).
- [35] J. E. Rice *et al.*, *Phys. Rev. Lett.* **106**, 215001 (2011).
- [36] J. E. Rice *et al.*, *Nucl. Fusion* **41**, 277 (2001).
- [37] J. E. Rice *et al.*, *Plasma Phys. Controlled Fusion* **50**, 124042 (2008).
- [38] P. J. Catto, *Phys. Fluids* **21**, 147 (1978).